

¹ Data Descriptor for Nature Scientific Data

² Carmen Cabrera-Arnau^{1,*}, Francisco Rowe¹, Miguel Gonzlez-Leonardo², Andrea
³ Nasuto¹, and Ruth Neville¹

⁴ ¹Geographic Data Science Lab, Department of Geography and Planning, University of Liverpool, Liverpool, UK

⁵ ²Centre for Demographic Urban and Environmental Studies, El Colegio de Mexico, Ciudad de Mxico, Mxico

⁶ * c.cabrera-arnau@liverpool.ac.uk

⁷ ABSTRACT

⁸ COVID-19 triggered a reduction in the frequency and extent of people's movement. Existing evidence suggests that while the impact of the pandemic on mobility was widespread, the extent of this impact was unequally felt across socioeconomic groups in the early stages of the pandemic. Here, we find that the most deprived locations have experienced a more accelerated recovery towards pre-pandemic levels of mobility in the long term. Furthermore, the socioeconomic disparities in the patterns of mobility triggered by the first outbreak of COVID-19, have persisted as of April 2023. These findings are based on the analysis of time-series mobility data corresponding to X urban areas from Latin American countries collected from Meta-Facebook users upon their consent. Our research highlights the importance of timely mobility data with high spatiotemporal resolution to understand the long-term effects of the pandemic and to inform equitable policy responses that address societal challenges in urban areas.

⁹ Main

¹⁰ @Francisco to rewrite this section

¹¹ Spatial human mobility is key to creating sustainable, livable and inclusive cities. At the societal level, spatial mobility enables the transfer of knowledge, skills and labour to places they are needed (Ackers 2005). Spatial mobility also shapes service and transport demand across urban spaces (Chen et al. 2016), and enables the monitoring and control of transmissible diseases (Belik, Geisel, and Brockmann 2011). At the individual level, mobility enables people to access and achieve opportunities and aspirations in space (Klugman 2009). Understanding spatial human mobility is thus important to supporting appropriate policy responses to address societal challenges relating to carbon emissions, urban planning, service delivery, public health, disaster management and transport (Barbosa et al. 2018; Chinazzi et al. 2020).

¹⁹ The COVID-19 pandemic resulted in a notable decrease in mobility, particularly in cities (Nouvellet et al. 2021). Coupled with fears of contagion in crowded public spaces, nonpharmaceutical interventions to contain the spread of COVID19 prompted this decrease in the overall levels of mobility (Nouvellet et al. 2021; Rowe, González-Leonardo, and Champion 2023). Especially during lockdowns, mobility recorded reductions in the frequency, distance and time of trips in cities across the globe (Abdullah et al. 2020; Bonaccorsi et al. 2020; Abu-Rayash and Dincer 2020; Lee et al. 2023). Higher engagement with remote working, online schooling and shopping activity reduced the need to travel for work, education, shopping and leisure, hence giving rise to more geographically localised mobility patterns (Borkowski, Jadewska-Gutta, and Szmelter-Jarosz 2021).

²⁷ However, reductions in mobility levels were highly unequal reflecting existing socioeconomic inequalities in our societies (Chang et al. 2020). In most countries, affluent individuals tended to record the greatest drops in mobility levels as they are predominantly employed in knowledge-intensive jobs which can be done fully or partly remotely (Fraiberger et al. 2020; Bonaccorsi et al. 2020; Weill et al. 2020; Dueñas, Campi, and Olmos 2021; Santana et al. 2023). During the COVID-19 pandemic, the adoption of remote work reduced the need of commuting for knowledge-intensive, non-public facing jobs (Florida, Rodríguez-Pose, and Storper 2021). At the same time, individuals from less privileged socioeconomic backgrounds displayed less pronounced declines mirroring the nature of their work requiring public-facing, face-to-face interaction, and thus a requirement for daily work commutes (Dueñas, Campi, and Olmos 2021; Santana et al. 2023).

³⁶ Thus, while a growing body of empirical evidence has contributed to advancing our understanding of the impacts

37 of the COVID-19 pandemic on spatial mobility within cities, existing research has focused on more developed
38 countries and the immediate effects of the pandemic during 2020. Less is known about the longer term patterns
39 of resilience in urban mobility in less developed countries extending beyond this period (Rowe et al. 2023). Urban
40 spaces have changed considerably since then, from going through waves of high COVID-19 fatality, infections, school
41 and business closures to the removal of all COVID-19 restrictions as the UN World Health Organization (WHO)
42 declared an end to the pandemic as a public health emergency; yet, different configurations of hybrid working have
43 remained in the norm across many sector of the economy (Barrero, Bloom, and Davis 2021; Aksoy et al. 2022).
44 Thus, assessing the extent to which the level of mobility has returned back to the pre-pandemic baseline level across
45 socioeconomic groups is important to understand the potentially unequal long-term impacts of hybrid working.

46 A key barrier to monitor changes in geographic mobility patterns in less developed countries during and post the
47 COVID-19 pandemic has been the lack of suitable data (Rowe et al. 2023). Traditionally census and survey data have
48 been employed to analyse human mobility patterns in these countries (Green, Pollock, and Rowe 2021). Yet, these
49 data streams are not frequently updated and suffer from slow releases, with census data for example being collected
50 over intervals of ten years in most countries (Bell et al. 2014). Traditional data streams thus lack the temporal
51 granularity to analyse population movements over short-time periods and to offer an up-to-date representation of
52 the urban mobility system (Rowe 2023b). Data resulting from social interactions on digital platforms have emerged
53 as an unique source of information to deliver this representation and capture human population movement in less
54 developed countries at scale (Rowe 2023b). Particularly location data from mobile phone applications have become
55 a prominent source to sense patterns of human mobility at higher geographical and temporal resolution in real time
56 (Calafiore et al. 2023).

57 Drawing on a dataset of 213 million observations from Meta-Facebook users' mobile location data, we aim to assess
58 socioeconomic differences in the extent and persistence of decline in urban mobility in Argentina, Chile, Colombia
59 and Mexico during and after the COVID-19 pandemic from March 2020 to March 2023. We use Meta-Facebook
60 data to measure origin-destination flows from March 2020 to May 2022, and Meta Prophet time-series forecasting
61 machine learning algorithm (Taylor and Letham 2017) to predict origin-destination flows from June 2022 to March
62 2023. We use Functional Urban Areas (FUAs) boundaries from the Global Human Settlement Layer (GHSL),
63 developed by the European Comission's Joint Research Centre (Schiavina M. 2019) to define urban areas; and the
64 Global Gridded Relative Deprivation Index (GRDI) developed by NASA's Socioeconomic Data and Applications
65 Centre (Columbia University 2022) from sociodemographic and satellite data inputs. Building on existing evidence
66 (e.g. Rowe et al. 2022; Wang et al. 2022), we hypothesised that (1) urban mobility has recovered returning to the
67 pre-pandemic baseline level of movement as nonpharmaceutical restrictions were lifted; and, that (2) socioeconomic
68 differences in urban mobility have endured the pandemic reflecting deep societal inequalities as knowledge-intensive
69 businesses adopt hybrid working.

70 Latin America provides an ideal test-bed for testing these hypotheses because of its exceptionally high levels of
71 inequalities (De Ferranti 2004; Carranza, De Rosa, and Flores 2023) and urbanisation (United Nations and Affairs.
72 2023). Half of the 20 most unequal countries in the planet are in this region. The average income Gini index of
73 the region is 4 percentage points higher than that of Africa and 11 higher than China (Milanovic 2016), and cities
74 display some of the steepest inequalities (Habitat 2022). Currently, over 80% of the population in Latin America
75 live in urban areas. By 2050, this share is predicted to reach 89%, with the largest share concentrating in a few
76 megacities (Habitat 2022). Developing an understanding of human mobility in Latin America is thus important to
77 support sustainable and inclusive spaces (Habitat 2022).

78 Results

79 We focus on capturing how mobility patterns for different population groups have been impacted by COVID-19 in
80 Latin America. We consider populations groups by classifying the spatial units of analysis into categories according
81 to their population density and their relative level of socioeconomic deprivation. More details for the classification
82 method are provided in the Methods section. The two criteria for classification are chosen due to their relevance
83 for *@Francisco, can you help here?*. The analysis of mobility is done using Facebook movement data that has
84 been processed according to our methodology.

85 **Affluent and densely populated areas saw steepest decline in daily mobility, but all population groups progress 86 towards baseline levels**

87 We first focus on analysing the variability in COVID-19's impact on daily mobility levels across different population
88 groups. Figure 1 shows changes in the intensity of movement measured as the percentage change in the number

89 of inflows relative to pre-pandemic baseline levels, at two key points during the period of analysis, May 2020 and
90 March 2022. These two months are the most widely spaced months with complete data available for all countries
91 within the period covered by the dataset. May 2020 represents the initial phase following the WHO's declaration
92 of COVID-19 as a global pandemic on March 11, 2020, marked by stringent measures. March 2022 represents
93 a later phase, roughly six months after most restrictions had been lifted in the countries included in the analysis.
94 Figure 1 presents boxplots depicting the distribution of percentage change in movement counts across areas grouped
95 by population density and deprivation index. The boxplots show mobility changes for each category in May 2020
96 and March 2022, with baseline levels marked by the dotted line at $y = 0$. Values above this line indicate increased
97 mobility from pre-pandemic levels, while values below show a reduction. These changes show remarkably consistent
98 patterns across countries for both types of classification.

99 Focusing first on the patterns by population density category, we generally observe a decrease in the number of
100 inflows for all countries and most categories of analysis in the early pandemic days. The extent of this decrease
101 tends to be larger for high-density areas. Although the majority of areas saw a decline in mobility during May
102 2020, some locations actually recorded higher movement levels compared to the pre-pandemic period, particularly
103 in regions classified as low-density. In fact, some of these areas saw their mobility levels double, as indicated by
104 outliers with percentage change exceeding 100%. However, this does not imply that these areas correspond to large
105 population numbers, as low-density regions typically contain very few residents, meaning that minor fluctuations in
106 population can lead to significant percentage change. Nonetheless, these relative changes illustrate the extent of the
107 impacts experienced by these sparsely populated regions. In March 2022, nearly two years later, mobility levels have
108 generally rebounded closer to pre-pandemic baseline levels across different population density categories. Notably,
109 mobility levels in areas characterised by higher population density still remain below the baseline. Low-density
110 areas show even greater variability than during the early days of the pandemic, with mobility levels often exceeding
111 the baseline. These high variability in sparsely populated regions may reflect the ongoing effects of the pandemic
112 on mobility, but they could also be influenced by seasonal variation (e.g. March compared to May). Overall, the
113 observed patterns by population density category are consistent with those reported in (Rowe et al. 2024) for
114 Argentina and Chile, where data from the same source corresponding to those two countries was analysed without
115 applying the data processing methodology proposed in this study.

116 Moving to the patterns by relative deprivation index category, we observe tendencies that mirror the patterns by
117 population density category. Firstly, in March 2020, there is an overall decrease in the number of inflows for all
118 countries and most categories of analysis. Exceptions to this general tendency notably occur in the most deprived
119 (less affluent) areas, especially in Colombia, where mobility levels in some regions are actually above the baseline.
120 This decrease displays a gradient across categories of analysis whereby the more affluent an area is, the higher
121 the losses in the number of inflows. After almost two years, we find evidence for a general recovery of mobility
122 closer to baseline levels across groups regardless of how deprived they are. However, disparities between groups
123 are still visible, indicating that the pandemic has exacerbated behavioral differences among groups with varying
124 socioeconomic statuses.

125 *@Miguel, can you elaborate the following in the discussion? - The pattern that we observe in
126 this section can be attributed to... THIS GOES TO THE DISCUSSION*

127 **Initial drop in mobility drives intergroup variation in mobility levels, as recovery pace is uniform across population 128 groups**

129 Next we focus on modelling intergroup differences in mobility trends over time, highlighting the variability in
130 the pace of recovery toward baseline mobility levels across population groups. Figure 2 and Figure 3 show, for
131 each country, the evolution over time in the intensity of movement, grouped into population density and relative
132 deprivation index categories respectively. Time is represented on the x -axis, spanning from mid-April 2020 to
133 mid-April 2022, while the intensity of movement is depicted on the y -axis, measured as the percentage change in
134 the number of flows relative to pre-pandemic baseline levels. The background of each plot in Figures Figure 2 and
135 Figure 3 is colored according to the stringency index, which quantifies the level of non-pharmaceutical interventions
136 implemented at each point in time to mitigate the spread of COVID-19, including measures such as social distancing
137 and lockdowns. This data provides context for the observed trends, reflecting the mobility restrictions imposed by
138 each country during the specified periods.

139 *@Francisco and @Miguel to check that what I wrote below makes sense*

140 We highlight four key observations from a visual inspection of the evolution patterns by population density category,

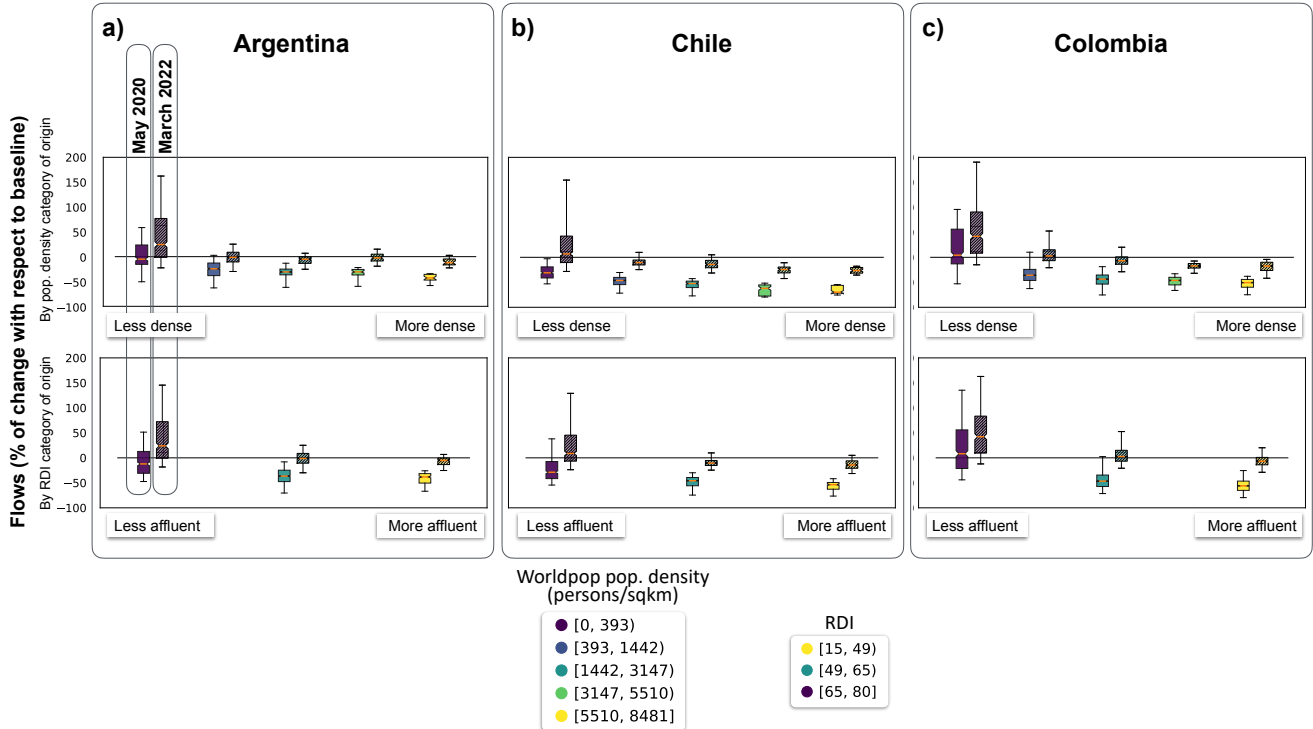


Figure 1. Changes in the intensity of flows as the percentage of change with respect to the pre-pandemic baseline levels, for each country and category of analysis at the origin location of each flow.

as shown in Figure 2. First, there is a general upward trend in mobility across all population density categories for all countries, reflecting a recovery of mobility levels following the early days of COVID-19. Second, more densely populated areas consistently record lower levels of mobility throughout the study period. Third, there exist some variations in the patterns by country. Chile experiences greater overall losses in mobility compared to Argentina, while certain areas in Argentina reach levels comparable to the pre-pandemic baseline. In contrast, Colombia displays more varied trends across population density categories, with above-baseline levels of mobility in low-density areas, and significantly larger losses in high-density areas. Fourth, the temporal patterns display fluctuations from the general trend. These fluctuations are likely driven by seasonality effects and by the changing levels of stringency of COVID-19 interventions.

Visual inspection of Figure 3 reveals the following four patterns by relative deprivation index category. First, we observe a general upward trend in mobility across all relative deprivation index categories for all countries. Second, less deprived areas consistently record lower levels of mobility throughout the study period. In contrast, more deprived areas exhibit higher levels of mobility. Third, there is variability by country. Colombia stands out for recording mobility levels in the most deprived areas that are well above the baseline. These big relative changes for the most deprived category do not necessarily correspond to large population numbers since for example, more deprived regions in Colombia are often low-density areas that typically contain small populations. As a result, minor fluctuations in mobility can lead to substantial percentage changes. Nevertheless, the positive percentage change observed in more deprived areas highlight the variability of the impact across different population groups based on their socioeconomic status. Fourth, like in Figure 2, the temporal patterns display fluctuations from the general trend which are likely driven by seasonality effects and by the changing levels of COVID-19 stringency index.

Next, we quantitatively model intergroup differences in mobility trends over Figure 2 and Figure 3. To achieve this, we perform a time series decomposition into three components: trend, seasonal, and residual. Our analysis focuses on the trend component, which we model using five specifications within a linear mixed-effects modeling framework, all yielding consistent results. All five models include time as a fixed effect and estimate an intercept and a slope associated with this variable. The intercept is interpreted as the magnitude of the initial drop in mobility, while the slope represents the rate at which mobility levels recover over time. Models 3, 4, and 5 incorporate random

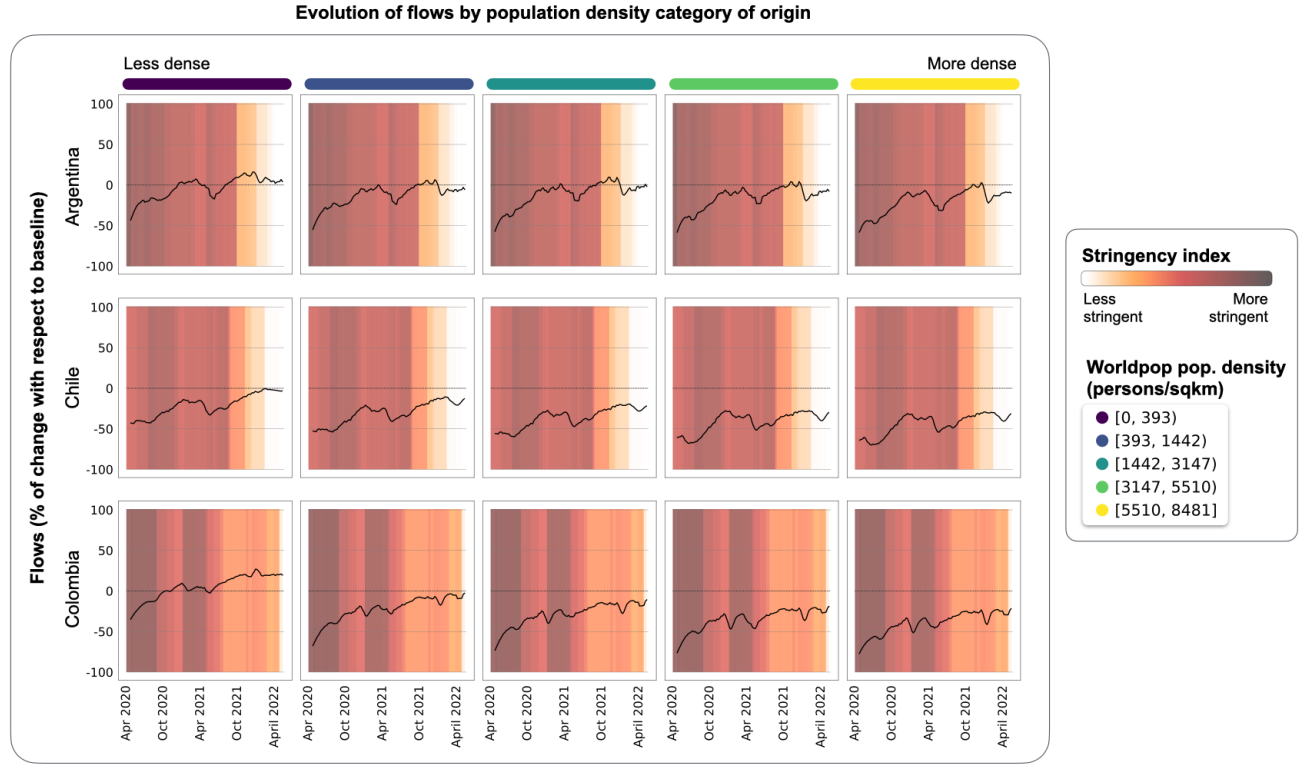


Figure 2. Evolution of number of flows by population density category of origin for Argentina, Chile and Colombia, as percentage change with respect to pre-pandemic baseline levels.

Evolution of flows by population density category of origin

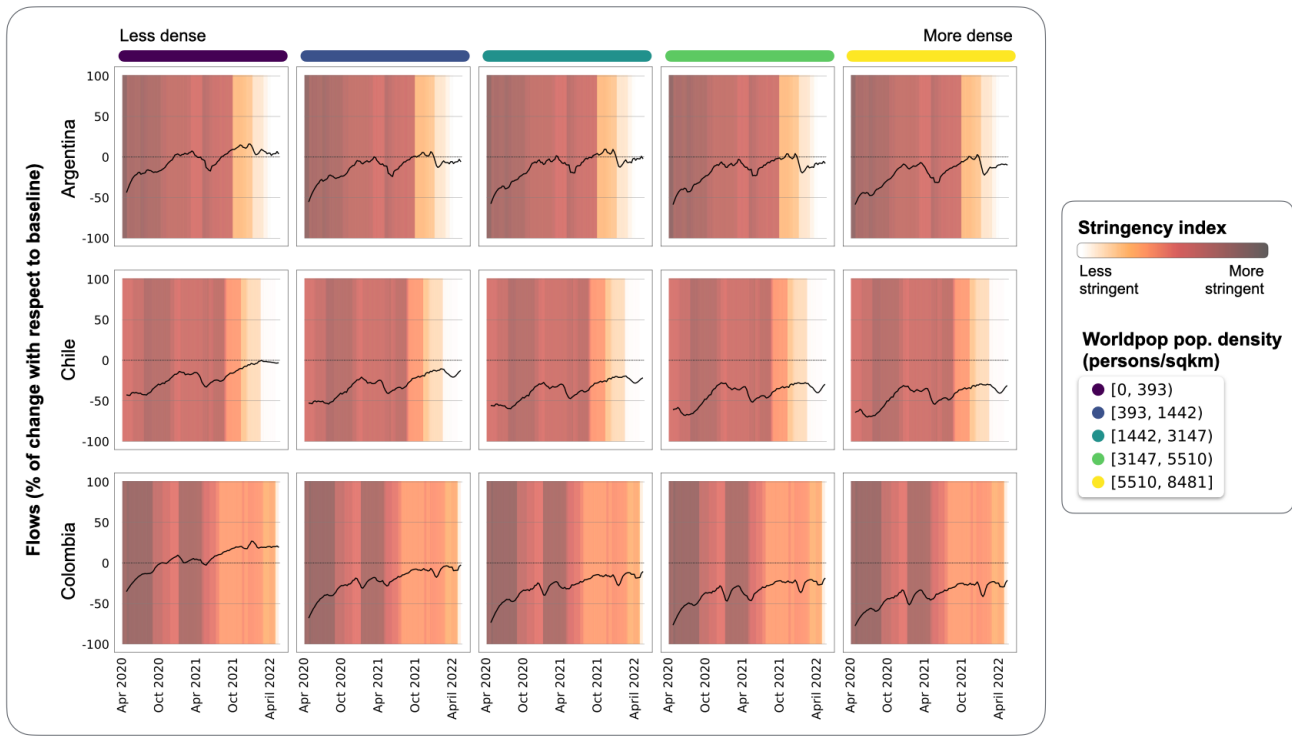


Figure 3. Evolution of number of flows by population density category of origin, as percentage change with respect to pre-pandemic baseline levels.

167 effects to capture variation in the intercept, slope, or both, based on the category of the origin of the flows. Detailed
 168 descriptions of all model specifications are provided in Methodology Section X.

169 Figures Figure 4 and Figure 5 present, for each country, the random variations in intercept and slope estimated
 170 by Models 3, 4, and 5, providing insights into the drivers of intergroup variation in the recovery towards baseline
 171 mobility levels. Focusing first on Figure 4, we observe that... *@Francisco to write this interpretation*

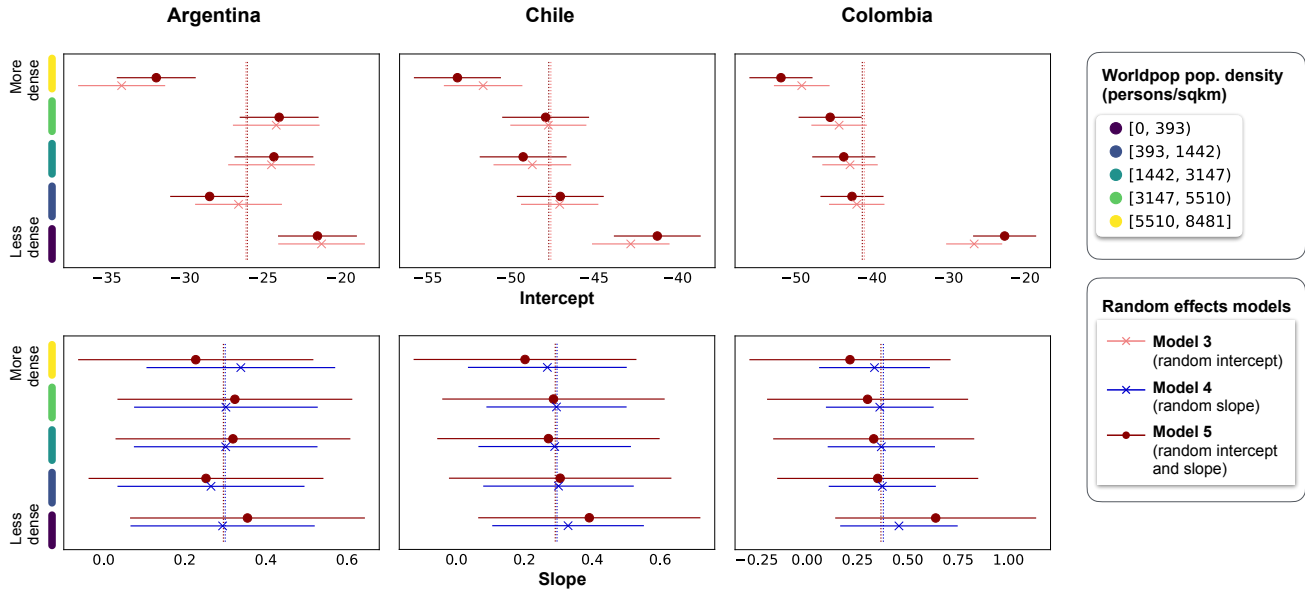


Figure 4. Figure random effects density

172 **Focus on cities - @Francisco @Miguel, we need a better title here - any ideas?**

173 Turning our focus to cities, we present a city-centric analysis of the evolution of movements. Specifically, we examine
 174 movements between urban centers and the rest of spatial units within each country, categorising these spatial units
 175 by population density to account for variability across the urban hierarchy. Urban centers are defined as the most
 176 densely populated spatial unit within each Functional Urban Area (FUA). The boundaries of these Functional
 177 Urban Areas are derived from the European Commission's Human Settlement Layer (GHSL) project (CEU. JRC.
 178 2019).

179 For each country, we analyze inflows to all FUA centers, considering two types of movements: those originating
 180 from any spatial unit (first column of Figure 6) and those from spatial units within a 100 km radius of the FUA
 181 centers (second column of Figure 6). Additionally, focusing only on urban centres corresponding to the capital
 182 FUAs -Buenos Aires, Santiago and Bogotá- we also look at inflows from any spatial unit and from those situated
 183 within a 100 km radius (columns third and fourth columns in Figure 6). The analysis is similarly repeated for
 184 outflows from urban centers to other spatial units.

185 *@Miguel to write this section. What can we learn about the figure? The target journal is nature
 186 cities, so we need to talk about cities...*

187 Discussion

188 *@Miguel to revisit this section - the text here was written a long time ago, before the analysis
 189 had taken the direction it's taken. Needs to be rewritten. Focus on trajectories of recovery.*
 190 *Focus on differences across population groups. Talk about remaining un-addressed biases in the
 191 data. With our methodology what we achieve is 1) data imputation for missing counts in regions
 192 that have low counts due to a variety of reasons -discuss- 2) data adjustment for fluctuations
 193 in daily number of users. However, our method does not explicitly adjust underrepresentation
 194 of specific population groups. This remains as future work and we should acknowledge the importance
 195 of this to make research based on digital traces more relevant for policy.*

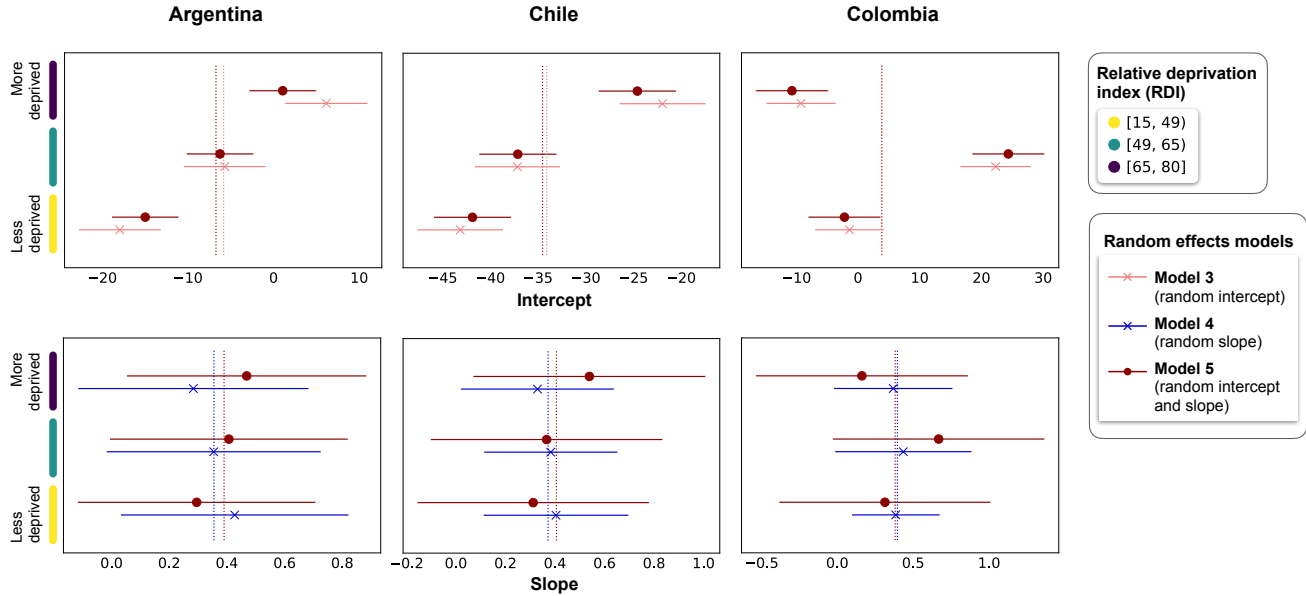


Figure 5. Figure random effects RDI

Using location data from Meta-Facebook users, our study aimed to examine the evolution of patterns of mobility across socioeconomic groups in functional urban areas from Argentina, Chile, Colombia and Mexico from April 2020 to March 2023, following the COVID-19 pandemic. We found a systematic drop in the number of population movements in April 2020, with the largest reductions observed in the most affluent administrative units within functional urban areas (FUAs) from Argentina, Chile and Colombia. While mobility rebounded closer to pre-pandemic levels approximately two years later, when COVID-19 restrictions eased, the number of movements remained below pre-pandemic in Chile. Furthermore, we found that at the beginning of the pandemic there were inequalities between socioeconomic groups in terms of the levels of urban mobility. While it has taken more than two years for Argentina and Mexico to gradually reduce gap, inequalities persist as of March 2023, especially in Chile and Colombia according to our estimated data.

We focused the analysis on short-distance movements in urban areas, specifically those covering 70 km or less. These journeys are typically considered to represent local and routine mobility (Owen and Green 1992). However, due to the characteristics of the Meta-Facebook movement data, we are unable to distinguish the purpose of these short-distance movements. Hence, some of our data could be capturing journeys that involve a permanent change of place of residence. Our work therefore motivates the need to answer questions regarding the validity of digital footprint data for the analysis of human mobility. Further research should focus on inferring more specific information about the nature of the journeys, following similar approaches to those proposed by Cabrera-Arnau et al. (2023), and quantifying the extent to which the digital footprint data mirrors the true mobility patterns.

Conducting research on urban mobility using digital footprint data is not straightforward, due to the challenges in accessing and working with unstructured data sets which are often subject to biases and statistical representation issues. These biases often arise from inequalities in access and usage of digital technologies across demographic groups (Rowe 2023a). Despite these challenges, the data and analysis that we used for this work provide evidence for non-trivial patterns that are consistent across four countries in Latin America and with other parts of the world. Our findings highlight the dynamic interplay between socioeconomic status and urban mobility, and shall be used to motivate and inform the public debate regarding the deep societal consequences of urban mobility disparities on the wider socioeconomic landscape of Latin American countries.

In conclusion, we argue that this work goes beyond the analysis of specific patterns by demonstrating the potential of digital footprint data for policy-relevant research on human mobility at an unprecedented level of spatiotemporal granularity. While we have seen a rise in initiatives to improve data services and methodological frameworks to facilitate the use of digital footprint data for social good, progress is still limited, especially in some parts of the world including Latin America. It is in the hands of governments and public organisations to prioritise the maximisation

Evolution of in/outflows to/from FUA centres (or capital), by population density category of origins/destinations

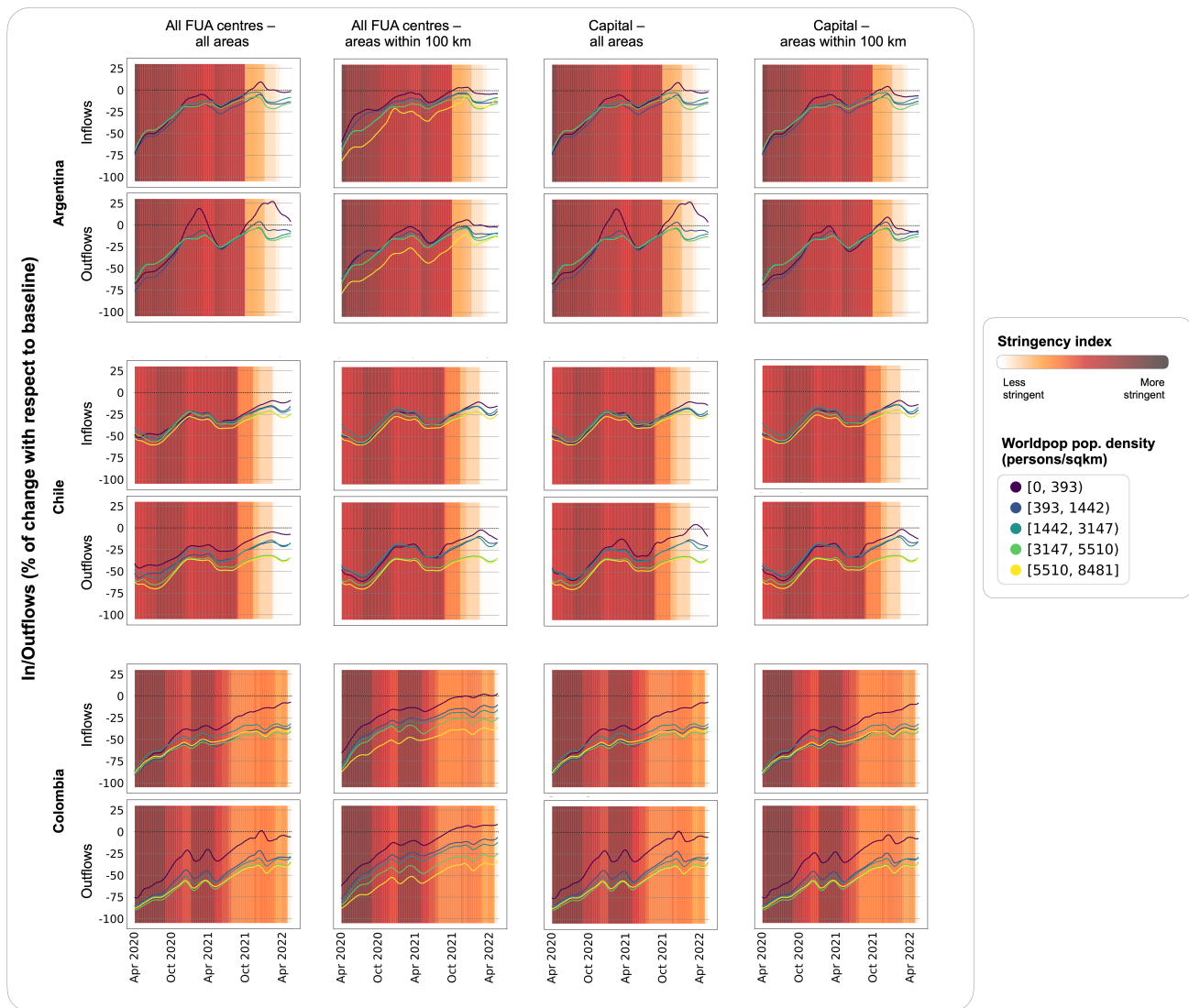


Figure 6. Evolution of number of inflows (and outflows) to (from) functional urban area centres, by population density category of origin (destination) for Argentina, Chile and Colombia, as percentage change with respect to pre-pandemic baseline levels.

the societal benefits that digital footprint data has to offer. This includes engaging in activities such as building strategic partnerships with commercial data-holders and academic institutions to establish a unified framework for the use of digital footprint data in policy and research. In particular, we call for the creation of resources like those developed by the European Commission Joint Research Centre (Commission et al. 2022) and the UN Statistics Division (Division 2019), which identify sources of non-traditional data and set methodological protocols for incorporating mobile phone data into official mobility statistics. While current resources tend to have a global reach, we advocate for more tailored local initiatives that acknowledge disparities in regional data availability and adoption of digital technologies.

235 Data

236 Meta-Facebook data

237 Facebook Movements

238 To capture population movements, we used anonymised aggregate mobile phone location data from Meta users for
 239 Argentina, Colombia and Chile, covering a 24-month period from April 2020 to March 2022. We used the Facebook
 240 Movements datasets created by Meta and accessed through their Data for Good Initiative (<https://dataforgood.facebook.com>). The data are built from Facebook app users who have the location services setting turned on
 241 on their smartphone. Prior to releasing the datasets, Meta ensures privacy and anonymity by removing personal
 242 information and applying privacy-preserving techniques (Maas et al. 2019). One such technique involves adding a
 243 small, undisclosed amount of random noise to prevent the determination of precise counts for these areas. Another
 244 technique consists in applying spatial smoothing, using inverse distance-weighted averaging, to create a smoother
 245 data surface. Finally, small-count dropping is applied to exclude records where the data counts are below 10.

246 The Facebook Movements datasets provide information on the aggregated number of Facebook app users moving
 247 between pairs of locations, during the 24-month crisis period during COVID-19. The data is spatially aggregated
 248 into tiles according to the Bing Maps Tile System developed by Microsoft (rbrundritt). The Facebook Movement
 249 data for Argentina, Chile and Colombia are spatially aggregated into Bing tile levels 13... respectively *@Carmen*
 250 *to check Bing Tile levels for movement data*. That is about 4.9 x 4.9km at the Equator (Maas et al. 2019).
 251 The data is temporally aggregated into three daily 8-hour time windows which are 00:00-08:00, 08:00-16:00 and
 252 16:00-00:00, Pacific Time (PT). These time windows translate to 05:00-13:00, 13:00-21:00, 21:00-05:00 for Argentina
 253 and Chile; and 03:00-11:00, 11:00-19:00, 19:00-03:00 for Colombia. For each time window, the origin location of a
 254 user is defined as the most frequently visited location in the previous time window, while the destination location
 255 is the most frequently visited location in the current time window.

256 In addition, each dataset includes baseline movement counts, which represent the estimated number of people
 257 moving prior to COVID-19. These baseline counts are calculated based on a 45-day period ending on March 10,
 258 2020, using the average for the same time of day and day of the week within this period. For example, the baseline
 259 for the 00:00-08:00 (PT) window on Mondays is calculated by averaging all Monday records for that time window
 260 across the 45-day period. Further details about the baseline can be found in (Maas et al. 2019).

261 Due to the small-count dropping privacy measure, movement counts during both the crisis and baseline periods
 262 are excluded if they fall below 10. However, even when counts are not reported, the datasets consistently provide
 263 the percentage change in movement counts relative to the baseline. This percentage change, denoted as $y_{ijdt}^{\%}$, is
 264 computed as follows (Maas et al. 2019):

$$y_{ijdt}^{\%} = \frac{y_{ijdt}^c - y_{ijdt}^b}{y_{ijdt}^b} \times 100.$$

265 Here, y_{ijdt}^c and y_{ijdt}^b represent the crisis and baseline movement counts, respectively, between origin tile i to
 266 destination tile j on day d and during time window t . For the baseline values y_{ijwt}^b , the subindex w denotes the
 267 day of the week corresponding to day d , as the baseline values are recorded by weekday, not by specific date. A
 268 small constant, usually set to 1, is added to the denominator to avoid division by zero (Maas et al. 2019).

269 Facebook Populations

270 As part of our proposed data processing methodology, we also utilize the Facebook Population datasets. Like the
 271 Facebook Movements data, these datasets cover a 24-month period from April 2020 to March 2022 and provide

273 information on the number of active Facebook users at specific locations during the crisis period.

274 The Facebook Population data is aggregated spatially into Bing tiles and temporally into 8-hour time windows. A
275 user's location is defined as the most frequently visited location within each 8-hour time window. Similar to the
276 Facebook Movements datasets, the Population datasets include baseline counts, calculated by averaging values for
277 the same day of the week and time of day over the 45-day pre-pandemic baseline period.

278 The same privacy-preserving techniques are applied to the Facebook Population datasets. As a result, population
279 counts during both the crisis and baseline periods are excluded if they fall below 10. However, the datasets
280 consistently report the percentage change in active user counts relative to the baseline. For tile i , day d and time
281 window t , the relative change in active user counts $p_{idt}^{\%}$ is computed as:

$$p_{idt}^{\%} = \frac{p_{idt}^c p_{iwt}^b}{p_{iwt}^b} \times 100,$$

282 where p_{idt}^c and p_{iwt}^b represent the crisis and baseline active user counts at tile i on day d and during time window
283 t . Once again, the subindex w in baseline values p_{iwt}^b denotes the day of the week corresponding to day d , and is
284 a small constant usually set to 1, added to the denominator to avoid division by zero (Maas et al. 2019).

285 In the remainder of the paper, we sometimes use expressions such as the “Facebook population” or the “population
286 of Facebook users” to refer to the number of active Facebook app users.

287 **Meta-Facebook data pre-processing**

288 For our analysis, we filter the data to include only one time window per day: 08:00–16:00 Pacific Time (PT), which
289 corresponds to 13:00–21:00 in Argentina and Chile, and 11:00–19:00 in Colombia. This window is likely to capture
290 the bulk of socioeconomic daytime activity, as well as a significant portion of morning commutes. The choice of
291 considering only one time window per day is driven by the objective of analysing the evolution of movement patterns
292 throughout the pandemic period, without focusing on variations through the day. By limiting the analysis to a
293 single time window each day, we reduce potential noise and variability that could arise from considering multiple
294 time windows per day. Furthermore, including all time windows could result in opposing movement trends that
295 may cancel each other out when the data is aggregated by day. As a result of filtering the data to include only one
296 time window per day, we can drop the subindex t from the variables defined above $y_{ijd}^{c,b,\%}$ and $p_{ijd}^{c,b,\%}$, as the time
297 window is no longer a distinguishing factor in the analysis.

298 As a pre-processing step, we ensure that both the Facebook movement and population data are aligned in terms of
299 spatial resolution for each country. Since the raw Facebook Population datasets are aggregated at a finer spatial
300 resolution, we re-aggregate them to match the spatial resolution of the Facebook Movements data.

301 **WorldPop population data**

302 We used data from WorldPop (Tatem 2017) to classify the spatial units of analysis according to their population
303 density, and to estimate missing baseline values in the Facebook population data. WorldPop offers open access
304 gridded population estimates at a resolution as small as 3 arc-seconds approximately 100m and 1km at the Equator,
305 respectively. WorldPop produces these gridded datasets using top-down (i.e. disaggregating administrative area
306 counts into smaller grid cells) or bottom-up (i.e. interpolating data from counts from sample locations into grid
307 cells) approaches. For the purposes of this work, we use gridded population data at a resolution of 1km² in raster
308 format. We perform a spatial join of the Facebook spatial units (Bing tiles) with the gridded population data and
309 compute the sum of Worldpop populations corresponding to each of the Facebook spatial units.

310 **Socioeconomic deprivation data**

311 We use the Global Gridded Relative Deprivation Index (GRDI), Version 1 (GRDIV1) (Columbia University 2022)
312 data set as a measure of socioeconomic deprivation. The GRDI data is made available via NASA’s Socioeconomic
313 Data and Applications Centre (SEDAC), at a spatial resolution of 30 arc-seconds, or 1 km² approximately. The
314 index quantifies the relative levels of multidimensional deprivation and poverty, where a value of 100 represents the
315 highest level of deprivation and a value of 0 the lowest. We perform a spatial join of the Facebook spatial units and
316 the gridded relative deprivation data and compute the average RDI corresponding to each of the Facebook spatial
317 units.

318 **Methods**

319 @Francisco to revise the whole section

320 **Processing Facebook data**

321 A significant challenge in analysing population counts and movements using Facebook user data is the absence of
 322 records for small counts. This limitation stems from privacy-protection measures designed to prevent the identifi-
 323 cation of individuals or small groups based on their location. The missing data in the Facebook Movements and
 324 Facebook Population datasets are not distributed randomly. Spatially, these missing values display high spatial
 325 autocorrelation as shown in Supplementary Figure ?@fig-autocorrelation for the Facebook Population datasets.
 326 Furthermore, due to the non-random nature of these missing values, spatial units that are sparsely populated or
 327 that have a low number of Facebook app users could potentially be underrepresented in the analysis. Therefore,
 328 simply removing the missing records from the analysis could lead to geographically biased results (Afghari et al.
 329 2019). To address this, we designed a data processing method for missing data imputation. An overview of this
 330 data imputation method is provided in Figure 7.

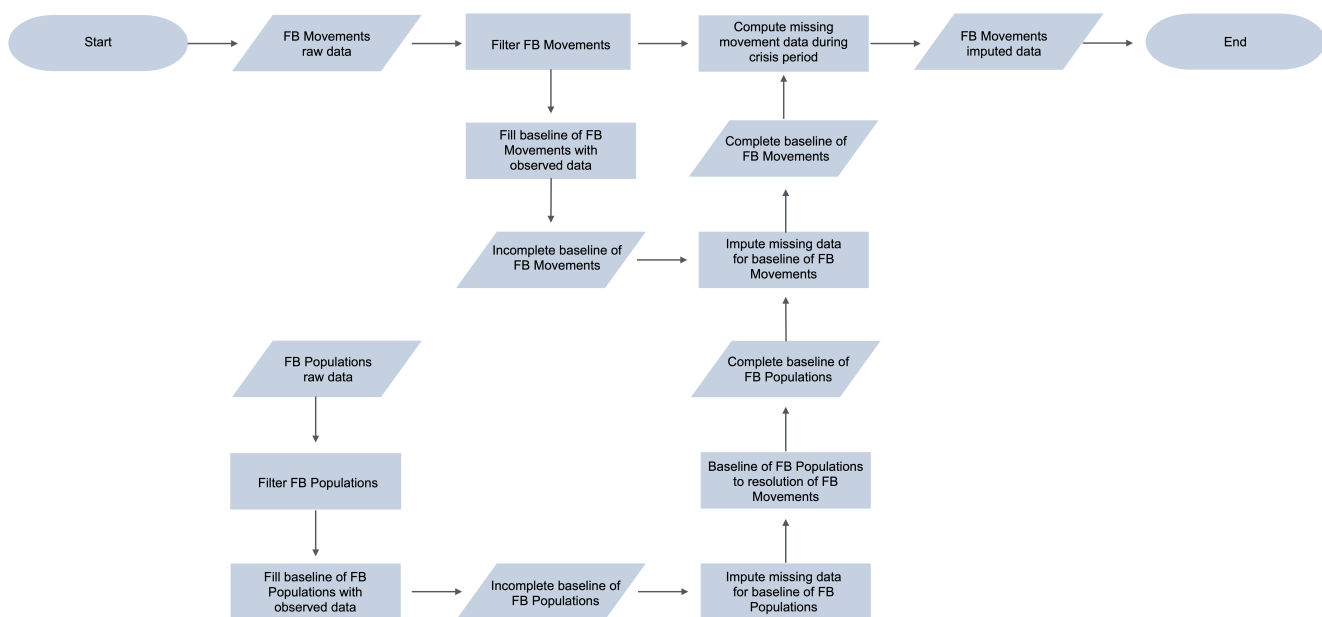


Figure 7. Workflow diagram for data imputation method.

331 Additionally, we apply correction factors and time series smoothing to eliminate the fluctuations in the daily number
 332 of observations, assuming that the representativeness of Facebook data across spatial units remains stable during
 333 the study period. The steps of our data-processing workflow are further described in the next four subsections.

334 **Imputing Facebook Population data**

335 We begin by identifying all the baseline values reported in the Facebook Population datasets, which form the basis
 336 for creating a new dataset that includes all available baseline information. Next, following (Duan et al. 2024), we
 337 use linear models to estimate the missing Facebook population baseline counts based on Worldpop population data.
 338 These models are fitted using ordinary least squares regression, with Worldpop data as the explanatory variable
 339 and the available baseline counts from the Facebook Population dataset as the dependent variable. The estimation
 340 process and its accuracy are illustrated in Supplementary Figure ?@fig-imputbaselinepop.

341 We then use the complete baseline of Facebook population counts to compute missing Facebook population counts
 342 during the crisis period. This is possible because, as mentioned above, Meta reports the percentage change in the
 343 number of counts with respect to the baseline $p_{id}^{\%}$, even if the counts are not reported due to low value.

344 **Imputing Facebook movement data**

345 The imputation of Facebook movement baseline values is done according to a spatial interaction model (see e.g.
 346 (Rowe, Lovelace, and Dennett 2022)). We consider baseline movement counts y_{ijw}^b between pairs of origin i and

347 a destination j tiles on weekday w , and model this variable as a function of the Facebook population count at
 348 the origin tile on the same weekday, the Facebook population count at the destination on the same weekday and
 349 the distance between origin and destination. We also include indicator variables to capture the day of the week.
 350 Mathematically, this model can be expressed as

$$b_{ijw} = 0 + 1p_{iw}^b + 2p_{jw}^b + 3d_{ij} + 4w + \dots \quad (1)$$

351 where $b_{ijw} = E[y_{ijw}^b]$ is the expectation of the flow of people from tile i to tile j on the weekday w during the baseline
 352 period; 0 is an intercept, p_{iw}^b and p_{jw}^b are the Facebook population counts at the origin and destination on weekday
 353 w during the baseline period, d_{ij} is the distance between origin and destination, w is a series of indicator variables
 354 capturing the day of the week, and $0,1,2,3,4$ are model parameters to be estimated from the observed data. The
 355 error term is denoted by \dots . To estimate the model parameters, we used a Gaussian regression model, taking the log
 356 of the population at origin and at destination, and the log of the distance. Residual plots for the spatial interaction
 357 model are provided in the Supplementary Figure ?@fig-residualsim.

358 We compute missing Facebook movement counts during the crisis period by considering the complete Facebook
 359 movements baseline and the percentage change in the number of counts with respect to the baseline, which is
 360 reported in the Facebook Movements datasets even when the count is not reported due to its low value.

361 **Applying correction factors**

362 The total number of active users within a given time window exhibits daily fluctuations due to limitations in Internet
 363 connectivity and user data access options (Maas et al. 2019). Following (Yabe et al. 2020) and (Duan et al. 2024),
 364 we applied a correction factor to mitigate the potential impact of these daily fluctuations on the results, since they
 365 could mask the mobility trends. This approach assumes that the representativeness of Facebook data across spatial
 366 units remains consistent throughout the study period.

367 The adjusted number of movements between tile i and tile j on day d , y_{ijd} was obtained as:

$$y_{ijd} = k_d \text{E} y_{ijd}^c$$

368 where y_{ijd}^c is the original number of movements between tiles i and j on day d during the crises period and k_d is a
 369 correction factor computed as the median of the sum of active user counts across all days d divided by the sum of
 370 active user counts across all spatial units on day d . Mathematically,

$$k_d = \frac{\text{med}_d(i p_{id}^c)}{i p_{id}^c}.$$

371 **Time series smoothing**

372 A time series for each pair of origin-destination tiles was generated using data processed as described above. However,
 373 the resulting time series still contained missing values due to days when no data was reported for specific location
 374 pairs. To ensure continuity, we addressed this issue by imputing missing values within the time series, replacing
 375 them with the average of the nearest 15 observations within the time series. This number was chosen to provide an
 376 optimal balance between maintaining temporal proximity and ensuring sufficient data coverage.

377 Additionally, to reduce noise and highlight underlying trends that might be obscured by short-term fluctuations,
 378 we applied a rolling-average smoothing technique to the resulting time series. This approach was used in the time
 379 series presented in Figure 2, Figure 3 and Figure 6.

380 **Classification of tiles according to level of urbanisation and socioeconomic deprivation**

381 The geographic distribution of categories for each of the countries is displayed in Figure 8 for Argentina, Chile and
 382 Colombia respectively. Figure 8 also shows, for each country, the proportion of the population across the various
 383 analysis categories is presented, based on both Facebook population counts and Worldpop population estimates.
 384 The Facebook population counts reflect the average number of active users across all weekdays in the pre-pandemic
 385 baseline period.

386 In all three countries, notable discrepancies appear between the population distributions according to WorldPop
 387 and Facebook data. For instance, in Argentina and Chile, WorldPop data indicates a higher proportion of people
 388 living in low-density areas, suggesting that Facebook data underrepresents populations in these regions. Similarly,
 389 in these countries, Facebook data shows an overrepresentation of the most affluent socioeconomic group. While
 390 addressing this kind of representativity bias is beyond the scope of this paper, we recognise its significance and the
 391 importance of addressing it in future analyses. This issue is revisited in the Discussion section.

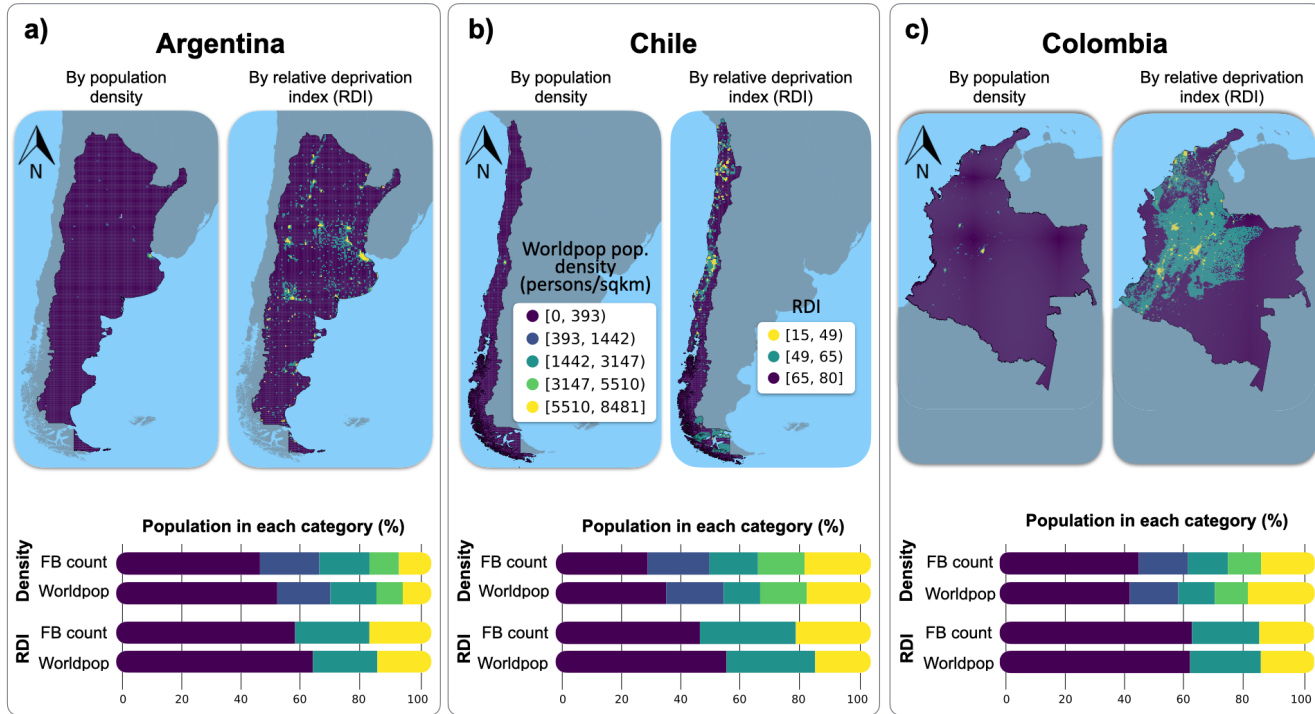


Figure 8. Classification of spatial units into categories by population density and by relative deprivation index. Spatial distribution of categories and population share in each category, by country.

392 Trend analysis

393 In order to quantify intergroup differences in the evolution towards pre-pandemic mobility patterns, we model the
 394 time series displayed in Figure 2 and Figure 3. To this end, we extract the trend, seasonal, and noise components
 395 of each time series using the `seasonal_decompose()` method from the time-series models and methods API in
 396 Python's `statsmodels` package (version 0.14.4). We then model the trend component according to five linear
 397 mixed-effects model specifications, using R's `glmmTMB` library (version 1.1.10).

398 Model 1 includes time as the sole explanatory variable, while Model 2 incorporates spatial heterogeneity by adding
 399 an indicator variable for the population density or RDI category of the origin. Models 3, 4, and 5 include time as
 400 a fixed effect but also incorporate random effects. Model 3 accounts for a random intercept based on the origin
 401 category, Model 4 includes a random slope for the origin category, and Model 5 combines both a random intercept
 402 and a random slope by origin category. Figures Figure 4 and Figure 5 illustrate the random variation in intercept
 403 and slope estimated by Models 3, 4, and 5. Full details on the parameter estimates are provided in Supplementary
 404 Tables (tab-trendanalysis?) for each country.

405 Code availability

406 For all studies using custom code in the generation or processing of datasets, a statement must be included under
 407 the heading “Code availability”, indicating whether and how the code can be accessed, including any restrictions
 408 to access. This section should also include information on the versions of any software used, if relevant, and any
 409 specific variables or parameters used to generate, test, or process the current dataset.

410 **References**

411 **Acknowledgements**

412 The work was supported by Research England..., project no. ... , 'RECAST'.

413 **Author information**

414 **Authors and affiliations**

415 **Contributions**

416 A.A. conceived the experiment(s), A.A. and B.A. conducted the experiment(s), C.A. and D.A. analysed the results.

417 All authors reviewed the manuscript.

418 **Ethics declarations**

419 **Competing interests**

420 The authors declare no competing interests.

421 **Supplementary information**

422 **Rights and permissions**

423 Springer Nature or its licensor (e.g. a society or other partner) holds exclusive rights to this article under a publishing
424 agreement with the author(s) or other rightsholder(s); author self-archiving of the accepted manuscript version of
425 this article is solely governed by the terms of such publishing agreement and applicable law.

426 Abdullah, Muhammad, Charitha Dias, Deepti Muley, and Md. Shahin. 2020. "Exploring the Impacts of COVID-19
427 on Travel Behavior and Mode Preferences." *Transportation Research Interdisciplinary Perspectives* 8 (November):
428 100255. <https://doi.org/10.1016/j.trip.2020.100255>.

429 Abu-Rayash, Azzam, and Ibrahim Dincer. 2020. "Analysis of Mobility Trends During the COVID-19 Coronavirus
430 Pandemic: Exploring the Impacts on Global Aviation and Travel in Selected Cities." *Energy Research & Social
431 Science* 68 (October): 101693. <https://doi.org/10.1016/j.erss.2020.101693>.

432 Ackers, Louise. 2005. "Moving People and Knowledge: Scientific Mobility in the European Union1." *International
433 Migration* 43 (5): 99–131. <https://doi.org/10.1111/j.1468-2435.2005.00343.x>.

434 Afghari, Amir Pooyan, Simon Washington, Carlo Prato, and Md Mazharul Haque. 2019. "Contrasting Case-Wise
435 Deletion with Multiple Imputation and Latent Variable Approaches to Dealing with Missing Observations in
436 Count Regression Models." *Analytic Methods in Accident Research* 24 (December): 100104. [https://doi.org/10.1016/j.amar.2019.100104](https://doi.org/10.
437 1016/j.amar.2019.100104).

438 Aksoy, Cevat Giray, Jose Maria Barrero, Nicholas Bloom, Steven Davis, Mathias Dolls, and Pablo Zarate. 2022.
439 "Working from Home Around the World." <https://doi.org/10.3386/w30446>.

440 Alexander, Lauren, Shan Jiang, Mikel Murga, and Marta C. González. 2015. "Origin–Destination Trips by Purpose
441 and Time of Day Inferred from Mobile Phone Data." *Transportation Research Part C: Emerging Technologies*
442 58: 240–50. <https://doi.org/10.1016/j.trc.2015.02.018>.

443 Barbosa, Hugo, Marc Barthelemy, Gourab Ghoshal, Charlotte R. James, Maxime Lenormand, Thomas Louail,
444 Ronaldo Menezes, José J. Ramasco, Filippo Simini, and Marcello Tomasini. 2018. "Human Mobility: Models
445 and Applications." *Physics Reports* 734 (March): 1–74. <https://doi.org/10.1016/j.physrep.2018.01.001>.

446 Barrero, Jose Maria, Nicholas Bloom, and Steven Davis. 2021. "Why Working from Home Will Stick." [https://doi.org/10.3386/w28731](https://
447 doi.org/10.3386/w28731).

448 Belik, Vitaly, Theo Geisel, and Dirk Brockmann. 2011. "Natural Human Mobility Patterns and Spatial Spread of
449 Infectious Diseases." *Physical Review X* 1 (1). <https://doi.org/10.1103/physrevx.1.011001>.

450 Bell, Martin, Elin Charles-Edwards, Dorota Kupiszewska, Marek Kupiszewski, John Stillwell, and Yu Zhu. 2014.
451 "Internal Migration Data Around the World: Assessing Contemporary Practice." *Population, Space and Place*
452 21 (1): 1–17. <https://doi.org/10.1002/psp.1848>.

453 Bonacorsi, Giovanni, Francesco Pierri, Matteo Cinelli, Andrea Flori, Alessandro Galeazzi, Francesco Porcelli,
454 Ana Lucia Schmidt, et al. 2020. "Economic and Social Consequences of Human Mobility Restrictions Under
455 COVID-19." *Proceedings of the National Academy of Sciences* 117 (27): 15530–35. [https://doi.org/10.1073/pnas.2007658117](https://doi.org/10.1073/
456 pnas.2007658117).

- Borkowski, Przemysaw, Magdalena Jadewska-Gutta, and Agnieszka Szmelter-Jarosz. 2021. "Lockdowned: Everyday Mobility Changes in Response to COVID-19." *Journal of Transport Geography* 90 (January): 102906. <https://doi.org/10.1016/j.jtrangeo.2020.102906>.
- Cabrera-Arnau, Carmen, Chen Zhong, Michael Batty, Ricardo Silva, and Soong Moon Kang. 2023. "Inferring Urban Polycentricity from the Variability in Human Mobility Patterns." *Scientific Reports* 13 (1): 5751. <https://doi.org/10.1038/s41598-023-33003-7>.
- Calafiore, Alessia, Krasen Samardzhiev, Francisco Rowe, Martin Fleischmann, and Daniel Arribas-Bel. 2023. "Inequalities in Experiencing Urban Functions. An Exploration of Human Digital (Geo-)footprints." *Environment and Planning B: Urban Analytics and City Science*, November. <https://doi.org/10.1177/23998083231208507>.
- Carranza, Rafael, Mauricio De Rosa, and Ignacio Flores. 2023. "Wealth Inequality in Latin America."
- CEU. JRC. 2019. *GHSL-OECD functional urban areas: public release of GHS FUA*. LU: Publications Office. <https://doi.org/10.2760/67415>.
- Chang, Serina, Emma Pierson, Pang Wei Koh, Jaline Gerardin, Beth Redbird, David Grusky, and Jure Leskovec. 2020. "Mobility Network Models of COVID-19 Explain Inequities and Inform Reopening." *Nature* 589 (7840): 82–87. <https://doi.org/10.1038/s41586-020-2923-3>.
- Chen, Cynthia, Jingtao Ma, Yusak Susilo, Yu Liu, and Menglin Wang. 2016. "The Promises of Big Data and Small Data for Travel Behavior (Aka Human Mobility) Analysis." *Transportation Research Part C: Emerging Technologies* 68 (July): 285–99. <https://doi.org/10.1016/j.trc.2016.04.005>.
- Chinazzi, Matteo, Jessica T. Davis, Marco Ajelli, Corrado Gioannini, Maria Litvinova, Stefano Merler, Ana Pastore y Piontti, et al. 2020. "The Effect of Travel Restrictions on the Spread of the 2019 Novel Coronavirus (COVID-19) Outbreak." *Science* 368 (6489): 395–400. <https://doi.org/10.1126/science.aba9757>.
- Columbia University, Center for International Earth Science Information Network. CIESIN. 2022. "Global Gridded Relative Deprivation Index (GRDI), Version 1." Palisades, New York: NASA Socioeconomic Data; Applications Center (SEDAC). <https://doi.org/10.7927/3xxe-ap97>.
- Commission, European, Joint Research Centre, C Bosco, S Grubanov-Boskovic, S Iacus, U Minora, F Sermi, and S Spyros. 2022. *Data Innovation in Demography, Migration and Human Mobility*. Publications Office of the European Union. <https://doi.org/doi/10.2760/027157>.
- De Ferranti, David M. 2004. *Inequality in Latin America: Breaking with History?* World Bank publications.
- Division, United Nations Statistical. 2019. "Handbook on the Use of Mobile Phone Data for Official Statistics."
- Duan, Qianwen, Jessica Steele, Zhifeng Cheng, Eimear Cleary, Nick Ruktanonchai, Hal Voepel, Tim O'Riordan, et al. 2024. "Identifying Counter-Urbanisation Using Facebook's User Count Data." *Habitat International* 150 (August): 103113. <https://doi.org/10.1016/j.habitatint.2024.103113>.
- Dueñas, Marco, Mercedes Campi, and Luis E. Olmos. 2021. "Changes in Mobility and Socioeconomic Conditions During the COVID-19 Outbreak." *Humanities and Social Sciences Communications* 8 (1). <https://doi.org/10.1057/s41599-021-00775-0>.
- Florida, Richard, Andrés Rodríguez-Pose, and Michael Storper. 2021. "Critical Commentary: Cities in a Post-COVID World." *Urban Studies* 60 (8): 1509–31. <https://doi.org/10.1177/00420980211018072>.
- Fraiberger, Samuel P., Pablo Astudillo, Lorenzo Candeago, Alex Chunet, Nicholas K. W. Jones, Maham Faisal Khan, Bruno Lepri, et al. 2020. "Uncovering Socioeconomic Gaps in Mobility Reduction During the COVID-19 Pandemic Using Location Data." <https://doi.org/10.48550/ARXIV.2006.15195>.
- Green, Mark, Frances Darlington Pollock, and Francisco Rowe. 2021. "New Forms of Data and New Forms of Opportunities to Monitor and Tackle a Pandemic." In, 423–29. Springer International Publishing. https://doi.org/10.1007/978-3-030-70179-6_56.
- Habitat, UN. 2022. "World Cities Report 2022: Envisaging the Future of Cities." *United Nations Human Settlements Programme: Nairobi, Kenya*, 41–44.
- Klugman, Jeni. 2009. "Human Development Report 2009. Overcoming Barriers: Human Mobility and Development." *Overcoming Barriers: Human Mobility and Development (October 5, 2009)*. UNDP-HDRO Human Development Reports.
- Lee, Sujin, Eunjeong Ko, Kitae Jang, and Suji Kim. 2023. "Understanding Individual-Level Travel Behavior Changes Due to COVID-19: Trip Frequency, Trip Regularity, and Trip Distance." *Cities* 135 (April): 104223. <https://doi.org/10.1016/j.cities.2023.104223>.
- Maas, P., S. Iyer, A. Gros, W. Park, L. McGorman, C. Nayak, and P. A. Dow. 2019. "Facebook Disaster Maps: Aggregate Insights for Crisis Response and Recovery." In *16th International Conference on Information Systems for Crisis Response and Management*, 836–47.
- Meng, Chuishi, Yu Cui, Qing He, Lu Su, and Jing Gao. 2017. "Travel Purpose Inference with GPS Trajectories,

- 512 POIs, and Geo-Tagged Social Media Data.” In *2017 IEEE International Conference on Big Data (Big Data)*,
513 1319–24. <https://doi.org/10.1109/BigData.2017.8258062>.
- 514 Milanovic, Branko. 2016. *Global Inequality: A New Approach for the Age of Globalization*. Harvard University
515 Press.
- 516 Nilufer Sari Aslam, Tao Cheng, Mohamed R. Ibrahim, and Yang Zhang. 2021. “ActivityNET: Neural Networks to
517 Predict Public Transport Trip Purposes from Individual Smart Card Data and POIs.” *Geo-Spatial Information
518 Science* 24 (4): 711–21. <https://doi.org/10.1080/10095020.2021.1985943>.
- 519 Nouvellet, Pierre, Sangeeta Bhatia, Anne Cori, Kylie E. C. Ainslie, Marc Baguelin, Samir Bhatt, Adhiratha
520 Boonyasiri, et al. 2021. “Reduction in Mobility and COVID-19 Transmission.” *Nature Communications* 12
521 (1). <https://doi.org/10.1038/s41467-021-21358-2>.
- 522 Owen, D., and A. Green. 1992. “Migration Patterns and Trends.” In *Migration Processes and Patterns: Research
523 Progress and Prospects*, edited by T. Champion and T. Fielding. Belhaven Press.
- 524 rbrundritt. “Bing Maps Tile System - Bing Maps — Learn.microsoft.com.” <https://learn.microsoft.com/en-us/bingmaps/articles/bing-maps-tile-system>.
- 525 Rowe, Francisco. 2023a. “9.: Big Data.” In *Concise Encyclopedia of Human Geography*, 42–47. Cheltenham, UK:
526 Edward Elgar Publishing. <https://doi.org/10.4337/9781800883499.ch09>.
- 527 ———. 2023b. “Big Data.” In *Concise Encyclopedia of Human Geography*, 42–47. Edward Elgar Publishing.
- 528 Rowe, Francisco, Carmen Cabrera-Arnau, Miguel González-Leonardo, Andrea Nasuto, and Ruth Neville. 2023.
529 “Reduced Mobility? Urban Exodus? Medium-Term Impacts of the COVID-19 Pandemic on Internal Population
530 Movements in Latin American Countries.” <https://doi.org/10.48550/ARXIV.2311.01464>.
- 531 ———. 2024. “Medium-Term Changes in the Patterns of Internal Population Movements in Latin American Coun-
532 tries: Effects of the COVID-19 Pandemic.” In *Population and Development Series*, No. 139 (LC/TS.2024/71).
533 Santiago: Economic Commission for Latin America; the Caribbean (ECLAC).
- 534 Rowe, Francisco, Alessia Calafiore, Daniel Arribas-Bel, Krasen Samardzhiev, and Martin Fleischmann. 2022. “Ur-
535 ban Exodus? Understanding Human Mobility in Britain During the COVID-19 Pandemic Using Facebook Data.”
536 <https://doi.org/10.48550/ARXIV.2206.03272>.
- 537 Rowe, Francisco, Miguel González-Leonardo, and Tony Champion. 2023. “Virtual Special Issue: Internal Migration
538 in Times of COVID-19.” *Population, Space and Place*, March. <https://doi.org/10.1002/psp.2652>.
- 539 Rowe, Francisco, Robin Lovelace, and Adam Dennett. 2022. “Spatial Interaction Modelling: A Manifesto.” <http://dx.doi.org/10.31219/osf.io/xcdms>.
- 540 Santana, Clodomir, Federico Botta, Hugo Barbosa, Filippo Privitera, Ronaldo Menezes, and Riccardo Di Clemente.
541 2023. “COVID-19 Is Linked to Changes in the Time-space Dimension of Human Mobility.” *Nature Human
542 Behaviour*, July. <https://doi.org/10.1038/s41562-023-01660-3>.
- 543 Schiavina M., Maffenini L., Moreno-Monroy A. 2019. “GHS-FUA R2019A - GHS Functional Urban Areas, Derived
544 from GHS-UCDB R2019A, (2015), R2019A.” European Commission, Joint Research Centre (JRC).
- 545 Tatem, Andrew J. 2017. “WorldPop, Open Data for Spatial Demography.” *Scientific Data* 4 (1). <https://doi.org/10.1038/sdata.2017.4>.
- 546 Taylor, Sean J, and Benjamin Letham. 2017. “Forecasting at Scale.” *PeerJ Preprints* 5 (September): e3190v2.
547 <https://doi.org/10.7287/peerj.preprints.3190v2>.
- 548 United Nations, Department for Economic, and Social Affairs. 2023. *World Population Prospects 2022: Summary
549 of Results*. UN.
- 550 Wang, Yikang, Chen Zhong, Qili Gao, and Carmen Cabrera-Arnau. 2022. “Understanding Internal Migration in
551 the UK Before and During the COVID-19 Pandemic Using Twitter Data.” *Urban Informatics* 1 (1). <https://doi.org/10.1007/s44212-022-00018-w>.
- 552 Weill, Joakim A., Matthieu Stigler, Olivier Deschenes, and Michael R. Springborn. 2020. “Social Distancing Re-
553 sponds to COVID-19 Emergency Declarations Strongly Differentiated by Income.” *Proceedings of the National
554 Academy of Sciences* 117 (33): 19658–60. <https://doi.org/10.1073/pnas.2009412117>.
- 555 Yabe, Takahiro, Kota Tsubouchi, Naoya Fujiwara, Takayuki Wada, Yoshihide Sekimoto, and Satish V. Ukkusuri.
556 2020. “Non-Compulsory Measures Sufficiently Reduced Human Mobility in Tokyo During the COVID-19 Epi-
557 demic.” *Scientific Reports* 10 (1). <https://doi.org/10.1038/s41598-020-75033-5>.